<Gamma Titanium Aluminides 2003> *<Edited by Kim,Clemens,Rosenberger>*
TMS (The Minerals, Metals & Materials Society, <2003>

SYNTHESIS OF NANO-CRYSTALLINE γ-TiAL MATERIALS

Stephen J. Hales and Peter Vasquez

NASA Langley Research Center
MS188A, 2 W. Reid St., Hampton, VA 23681, USA.

Abstract

One of the principal problems with nano-crystalline materials is producing them in quantities and sizes large enough for valid mechanical property evaluation. The purpose of this study was to explore an innovative method for producing nano-crystalline γ-TiAl bulk materials using high energy ball milling and brief secondary processes. Nano-crystalline powder feedstock was produced using a Fritsch P4^{TM} vario-planetary ball mill recently installed at NASA-LaRC. The high energy ball milling process employed tungsten carbide tooling (vials and balls) and no process control agents to minimize contamination. In a collaborative effort, two approaches were investigated, namely mechanical alloying of elemental powders and attrition milling of pre-alloyed powders. The objective was to subsequently use RF plasma spray deposition and short cycle vacuum hot pressing in order to effect consolidation while retaining nano-crystalline structure in bulk material. Results and discussion of the work performed to date are presented.

Introduction

The specific high temperature properties of gamma titanium aluminide (γ-TiAl) alloys make them attractive candidates for structural weight reduction on high-speed aircraft and reusable launch vehicles [1]. The potential exists for their use in hot structure or honeycomb core sandwich structure applications in sheet or foil product form [2]. However, the Achilles' heel to the widespread application of these materials has been their poor room temperature (RT) ductility and toughness. A processing philosophy with promise for improving the RT ductility of γ-TiAl alloys without sacrificing other desirable mechanical properties is extreme grain refinement. Previous studies have shown that reducing the grain size from 100 μm to 6 μm results in an increase in RT ductility [3], but a decrease in RT ductility (and other properties) has been observed when reducing the grain size from 200 nm to 10 nm [4, 5]. The difference in grain size between these two independent studies is approximately four orders of magnitude. The premise for the present work is that there may be a 'sweet spot' within the intermediate grain size range at which RT ductility can be optimized.

A versatile method for producing bulk nano-crystalline material involves the use of high energy ball milling for mechanical alloying of elemental powders or attrition milling of pre-alloyed powders [6]. This research represents a collaborative exercise between the University of Illinois (UIUC) and NASA Langley Research Center (LaRC). The focus of the present paper is the milling of pre-alloyed γ-TiAl powders at LaRC, since results from milling of elemental and pre-alloyed powders at UIUC have been presented previously [7]. The LaRC effort combines planetary ball milling and low pressure RF plasma spraying with vacuum hot pressing and heat treatment to produce a thin gage product. Control of the extent of microstructural coarsening,

routinely observed during consolidation of nano-crystalline powders [e.g. 8], is anticipated to yield bulk material with grain sizes in the desired range. Following the work of others, the target microstructure comprises a highly refined, fully lamellar grain structure for the best balance of mechanical properties [9].

Experimental Procedures

The Fritsch Pulverisette P4^{TM} vario-planetary ball milling facility at LaRC represents state-of-the-art equipment by being the first of a new series of planetary ball mills (PBM's) capable of independent control of the rotation speeds of the grinding vials and supporting disk (Figure 1(a)). On conventional PBM's the vials rotate and are mounted eccentrically on a rotating support disk. The rotation speed of the supporting disk can be selected and the vials rotate at a fixed transmission ratio. The transmission ratio controls the trajectories of the balls inside the vials and, thus, the milling energy. In the LaRC PBM the trajectories of the balls can be controlled to strike the inner wall of the vial perpendicularly (high impact energy), or approach tangentially (high friction energy) by varying the transmission ratio [10]. The relative rotation speed of the vials with respect to the supporting disk, or "vial to supporting disk" rotation speed ratio, is known as the R-ratio. For example, when R = -2.0, the grinding vials undergo two clockwise revolutions for each counter-clockwise revolution of the supporting disk (Figure 1(b)). The relative amounts of 'friction' vs. 'impact' processing can be controlled via manipulation of the R- ratio.

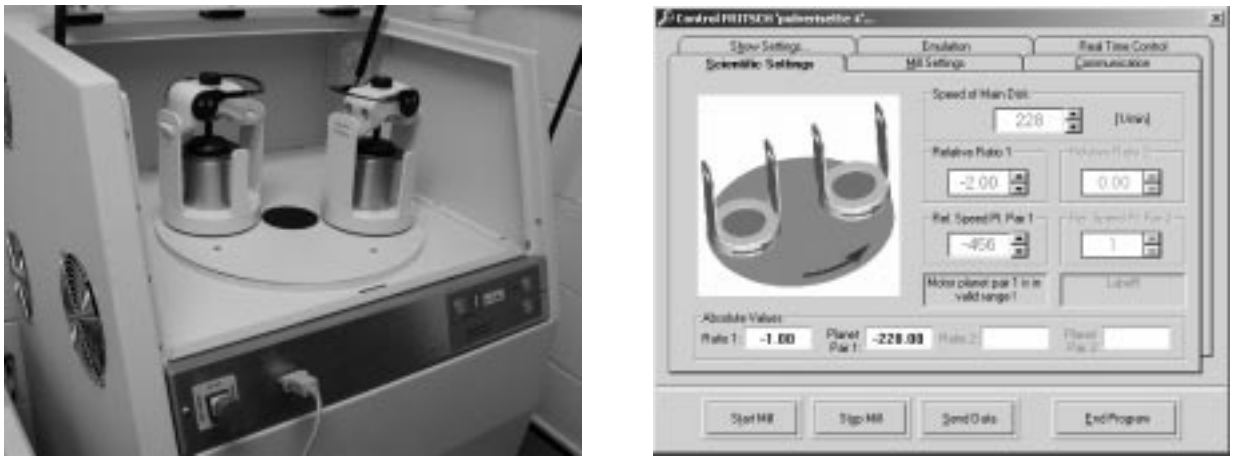

(a) **(b)**

Figure 1. Fritsch pulverisette P4^{TM} vario-planetary ball mill;
(a) tungsten carbide vials mounted on supporting disk
(b) software display used to control and monitor milling parameters

High energy ball milling experiments were conducted on pre-alloyed –35 to +80 mesh (180-512 μm diameter) powders with nominal composition Ti-46.5Al-2.5Cr-1.0Nb-0.5Ta-0.1B (at. pct.). Tungsten carbide vials and balls were employed and no process control agents (PCA's) were used. The capacity of each of the two vials was 250 ml and ball diameters (D_B) were selected from 20 mm, 9.5 mm (0.375 in.) and 6.4 mm (0.25 in.). The R-ratio was varied between –2.0 and +2.0 and the ball mass to powder mass ratio (M_B/M_P) varied between 5:1 and 15:1. With reference to the UIUC work, parameters for the baseline run in the present work comprised 400 g of 20 mm balls plus 40 g of powder (M_B/M_P = 10:1) with a supporting disk rotation speed of 228 rpm, an R-ratio of –2.0 and a milling time of 5 hrs. The milling process was interrupted after each hour to decant samples for analysis. The vials were purged with argon gas and powders were handled inside an argon-filled glove box. X-ray diffraction measurements provided phase identification and γ crystallite size (d_γ). The microstructure of the pre-alloyed

powders actually comprised a mixture of γ (f.c.t. TiAl) and α_2 (ordered h.c.p. Ti_3Al) phases. Scherrer's analysis of the $(111)_\gamma$ peak was used to estimate the γ crystallite size, as the predominant phase. Standard SEM/EDS practices were adopted for determining the size, morphology and composition of powders as a function of milling parameters.

Results and Discussion

Parametric studies conducted at UIUC, using a conventional PBM, were used to guide the LaRC effort. The first experiments were designed to duplicate the UIUC results, and subsequent experiments were designed to isolate the effects of selected variables by taking advantage of the enhanced capabilities of the LaRC PBM facility. The UIUC work indicated that the biggest problem with ball milling was sticking of the powders to the milling tools, i.e. balls and vial walls, necessitating frequent interruptions of the process to break up the 'clogging'. The logistics of breaking up these clogs are not trivial and has proven to be time consuming. Consequently, parametric studies at UIUC focused on 'time-to-clog' vs. milling media. Their results indicated that the shortest milling times were the most desirable from the perspective of minimizing clogging. The UIUC results also indicated that, without using PCA's, that tungsten carbide tooling was more effective than Cr-steel or C-steel tooling in producing nano-crystalline material. Therefore, only tungsten carbide vials and balls were employed in the present study.

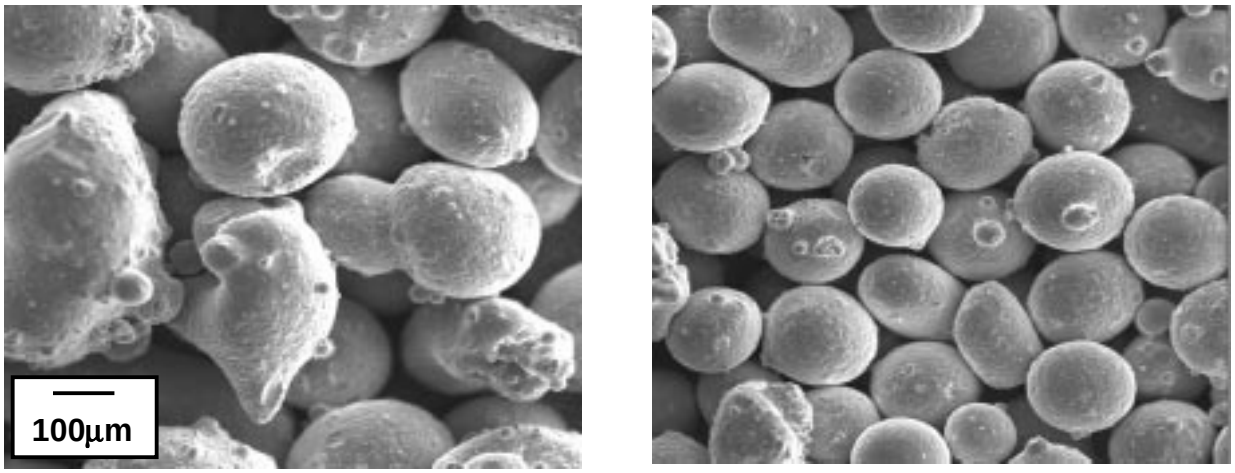

(a) **(b)**

Figure 2. Pre-alloyed γ-TiAl powder feedstock;
(a) -35 to +80 mesh (180-500 μm diameter) for high energy ball milling
(b) -80 to +140 mesh (106-180 μm diameter) for plasma spray deposition

Figure 2(a) illustrates the size and morphology of the spray atomized, pre-alloyed γ-TiAl powders prior to ball milling. It is apparent that the powder surfaces are smooth and the powder morphology is mostly spheroidal with evidence of some lobe and satellite formations. This powder is too coarse to be employed as plasma spray feedstock, since powders typically used fall in the –80 to +140 mesh (100-180 μm diameter) range, Figure 2(b). The effect of varying the R-ratio, R = +2.0, -1.0 and –2.0 (D_B = 20 mm, M_B/M_P = 10:1) on powder size and morphology following 5 hrs of milling is illustrated in Figure 3. Comparing Figure 3(a) with Figure 2(a) shows that using R = +2.0 causes little change in the overall size and morphology of the powders. The lobes and satellites have been removed, but the smooth surfaces persist. In contrast, Figures 3(b) and 3(c) show that using negative R-ratios results in fragmentation of the powders to much smaller dimensions and rougher surfaces (see Figures 3(b) and 3(c)).

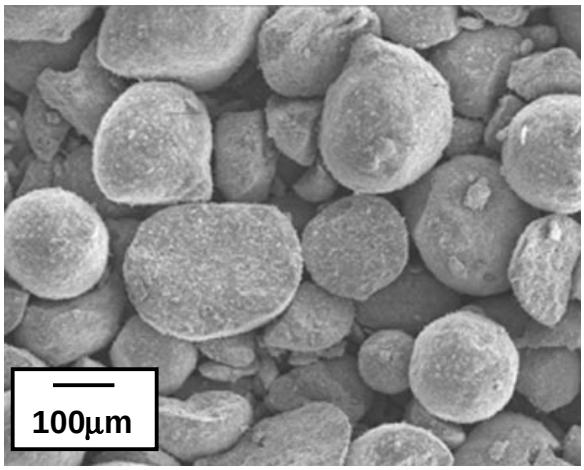

(a)

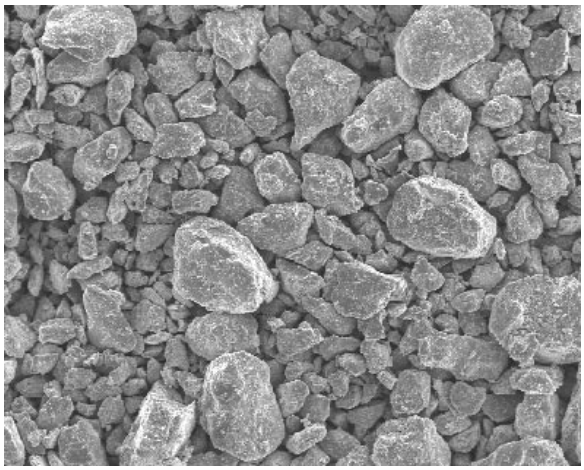

(b)

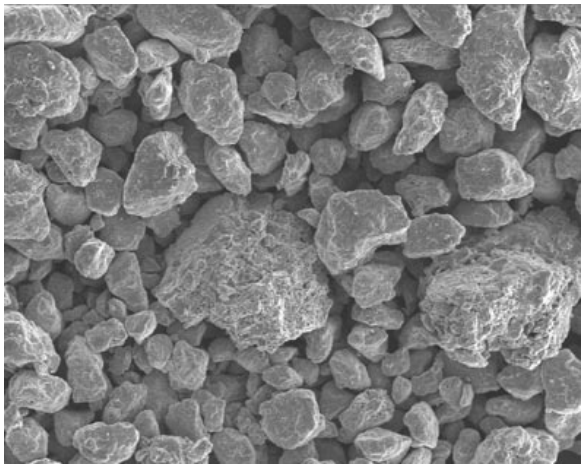

(c)

Figure 3. Effect of R-ratio on powder size and morphology;
(a) M_B/M_P= 10:1, D_B= 20 mm, R = +2.0
(b) M_B/M_P= 10:1, D_B= 20 mm, R = -1.0
(c) M_B/M_P= 10:1, D_B= 20 mm, R = -2.0

The effect of varying the ball diameter, D_B = 20 mm, 9.5 mm and 6.4 mm (R = -2.0, M_B/M_P = 10:1) on powder size and morphology following 5 hrs of milling is shown in Figure 4. A comparison of Figures 4(a) and 4(b) with Figure 3(c) reveals that decreasing D_B does not result in systematic changes in the powder size and morphology. The powders in Figure 4(a), milled using the intermediate (9.5 mm) ball size, do appear finer than the others. Figure 5 shows the effect of varying the ball mass to powder mass ratio, M_B/M_P = 5:1, 10:1 and 15:1 (R = -2.0, D_B = 20 mm) on powder size and morphology following 5 hrs of milling. Comparing Figures 5(a) and 5(b) with Figure 3(c) reveals that changing the M_B/M_P ratio also has no systematic effect on the powder size and morphology. The powders in Figure 5(b), milled using the highest M_B/M_P (15:1) ratio, do appear finer and more fragmented than the others. In combination, these observations suggest that changing the R-ratio from positive to negative values has the largest influence over the size and morphology of the powders during ball milling. The lesser effects of the varying the ball diameter, D_B, and the M_B/M_P ratio are less certain at present.

Scherrer's analysis of XRD data from the –35 to +80 mesh powders provided an estimate of the gamma crystallite size, d_γ = 20.0 nm prior to ball milling. The effect of varying the R- ratio, R = +2.0, -1.0 and –2.0 (D_B = 20 mm, M_B/M_P = 10:1) on d_γ is shown in Figure 6(a). Employing R = +2.0 results in a steady decrease in d_γ from 20.0 nm to 15.0 nm following 5 hrs of milling. Employing negative values of R-ratio results in a dramatic decrease in d_γ during the first hour of milling with a much smaller cumulative decrease over the remaining 4 hrs. Using R = -2.0 ultimately results in a smaller value of d_γ compared with R = -1.0, after 5 hrs of milling. Both

cases culminate in a finer gamma crystallite size than for R = +2.0, d_γ = 11.5 nm and d_γ = 12.6 nm, respectively.

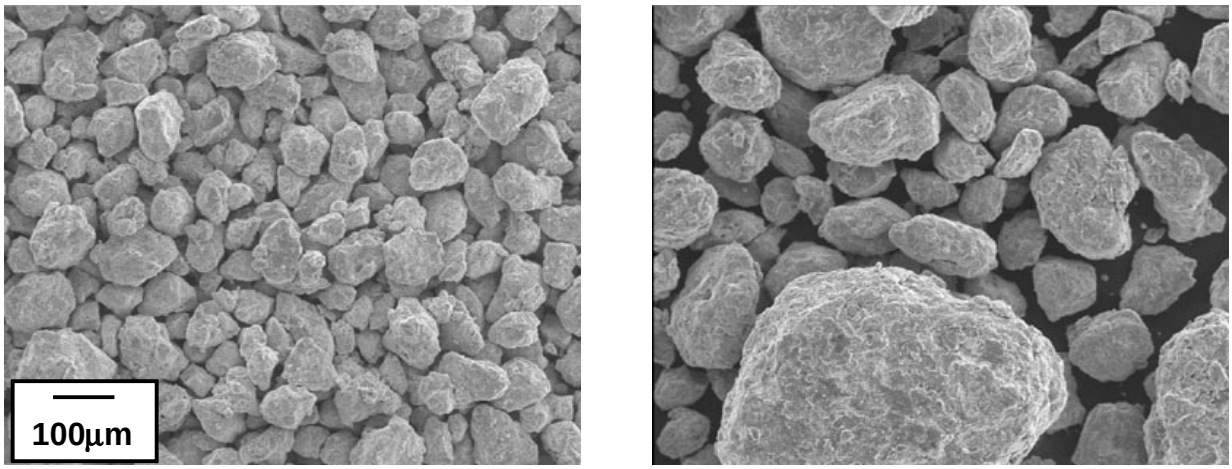

(a) **(b)**

Figure 4. Effect of ball diameter on powder size and morphology; (a), M_B/ M_P= 10:1, R = -2.0, D_B= 9.5 mm; (b), M_B/ M_P= 10:1, R = -2.0, D_B= 6.4 mm

Figure 6(b) shows the effect of varying the ball diameter, D_B = 20 mm, 9.5 mm and 6.4 mm (R = -2.0, M_B/M_P = 10:1) on d_γ. The plot relating to the 20 mm diameter balls is common with Figure 6(a). The data pertaining to the smaller diameter balls reveal that the rapid decrease in d_γ during the first hour is absent. However, after 5 hrs of milling the final d_γ values are reduced from 11.5 nm to 11.2 nm to 10.1 nm with decreasing ball diameter. The effect of varying the ball mass to powder mass ratio, M_B/M_P = 5:1, 10:1 and 15:1 (R = -2.0, D_B = 20 mm) on d_γ is shown in Figure 6(c). The plot relating to the 10:1 ball mass to powder mass ratio is common with Figures 6(a) and 6(b). Again the rapid decrease in d_γ after 1 hr of milling is only observed for M_B/M_P =10:1, the other two conditions exhibited a gradual decrease in d_γ over 5 hrs. Trends in the 5 hr data show that as the M_B/M_P ratio increased, d_γ decreased from 15.8 nm to 11.5 nm to 10.6 nm.

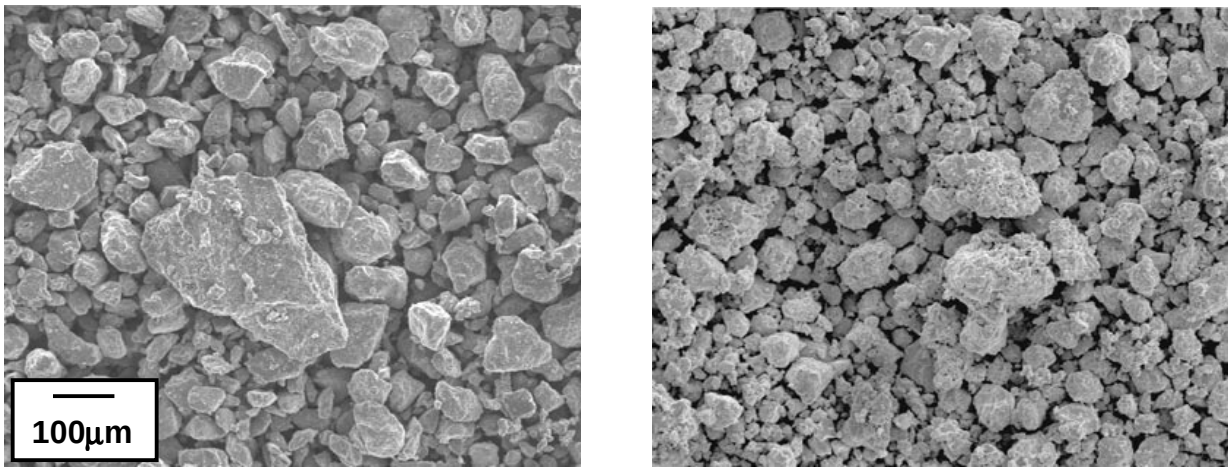

(a) **(b)**

Figure 5. Effect of ball mass to powder mass ratio on powder size and morphology; (a), R = -2.0, D_B= 20 mm, M_B/ M_P= 5:1; (b), R = -2.0, D_B= 20 mm, M_B/ M_P= 15:1

The data reveal that different milling parameters are appropriate based on whether the ultimate goal is to minimize γ crystallite size or to minimize milling time. If minimum d_γ is desirable

(using 5 hr milling times), then the following parameters would be selected: R = -2.0, D_B = 6.4 mm, M_B/M_P = 10:1; which yield d_γ = 10.1 nm. However, if a short milling time is desired (culminating in lesser microstructural refinement), then the following parameters would be selected for a 1hr milling time: R = -2.0, D_B = 20 mm, M_B/M_P = 10:1; which yield d_γ = 12.8 nm. Use of these parameters represents a 36 % decrease in gamma crystallite grain size after 1 hr versus a 50 % decrease after 5 hrs of milling.

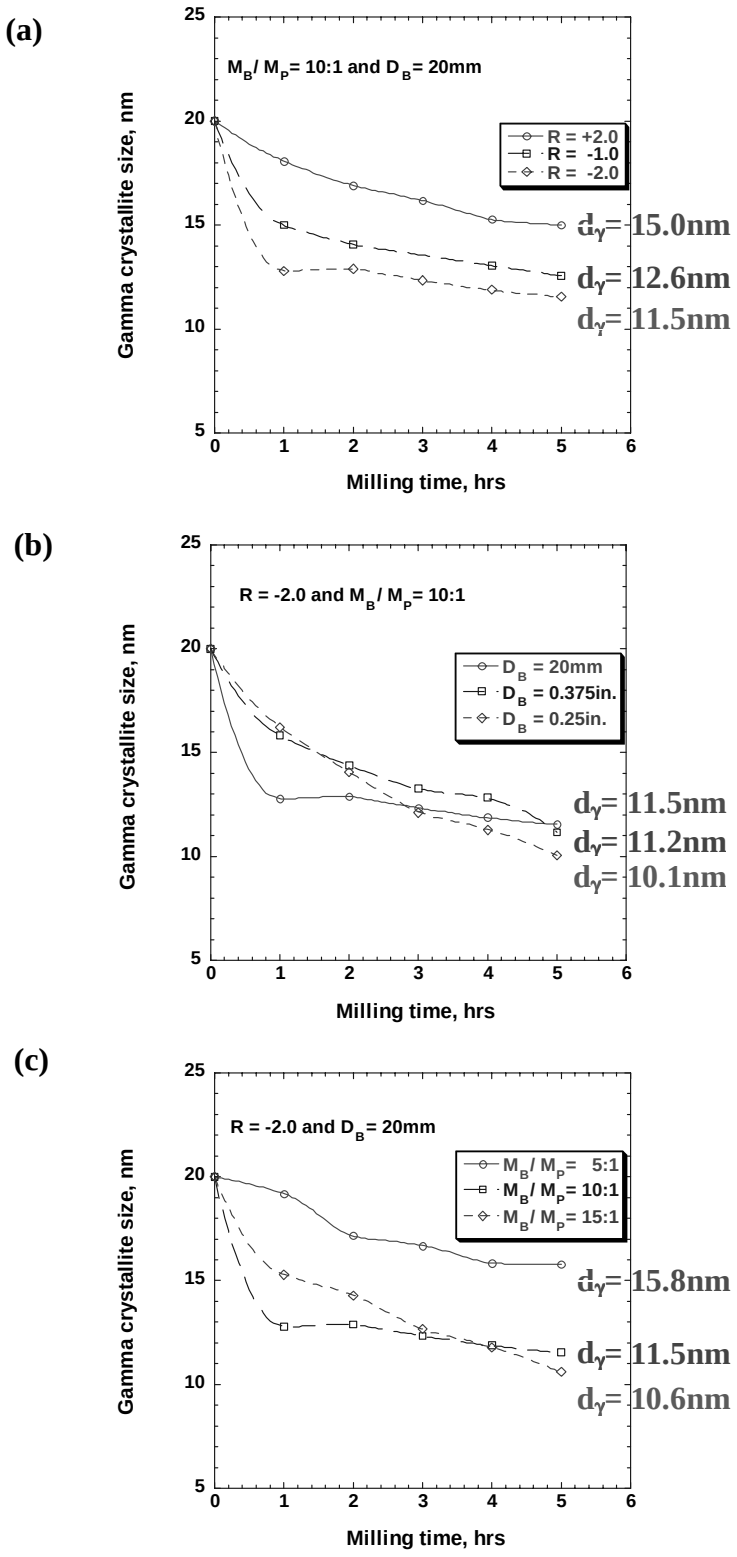

Figure 6. Effect of selected ball milling parameters on gamma crystallite size, d_γ; (a) R-ratio; (b) ball diameter, D_B; (c), ball mass to powder mass ratio, M_B/M_P

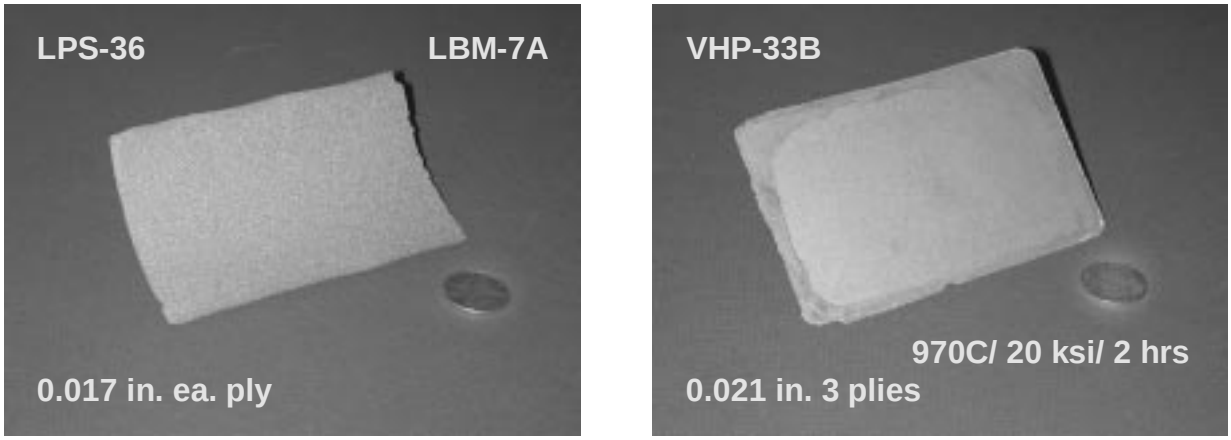

(a) **(b)**

Figure 7. Secondary processing of ball-milled powders to a 7.6 cm x 12.7 cm panel; (a), RF plasma spray deposited; (b), vacuum hot press consolidated

Although not addressed in detail in this paper, proof-of-concept studies were conducted with 5 hr ball-milled powders with a starting d_γ = 12.0 nm. Sufficient quantities were plasma sprayed to produce multiple plies of 7.6 cm x 12.7 cm x 0.43 mm thick deposit (Figure 7(a)), and subsequently 3 plies were consolidated via vacuum hot pressing to produce a 0.53 mm thick panel (Figure 7(b)). The gamma crystallite grain size was estimated via XRD to be 31.3 nm in the as-deposited condition and 90.0 nm in the as-consolidated condition. This suggests that the processing approach adopted has merit for producing bulk nano-crystalline materials. Another objective of this work was to minimize contamination by not employing PCA's etc. However, as shown in Table 1, contamination of the powders with tungsten and carbon from the tungsten carbide balls and vials was detected. The oxygen content is also higher than desirable from the perspective of being detrimental to mechanical properties. This issue has been noted by others during milling of hard materials [6], and alleviating this problem will be an important element of future work.

Table 1. Compositional variations during processing (wt. pct.)

Element	Starting Powder	As-deposited	As-consolidated
Ti	Bal.	Bal.	Bal.
Al	33.0	29.4	29.4
Cr	2.8	3.1	3.1
Nb	2.6	2.4	2.6
Ta	2.5	2.4	2.5
B	0.031	0.018	0.029
W	---	4.3	4.5
C	0.021	0.331	0.333
O	0.065	0.305	0.219
N	0.008	0.027	0.029
H	0.0046	0.0095	0.0007

Conclusions

- High energy ball milling of pre-alloyed **γ**-TiAl powders resulted in a reduction of the initial **γ** crystallite size, d_γ , for all milling conditions evaluated. The effect of selected variables following 5 hrs of milling was as follows :-
  (a) using D_B = 20 mm and M_B/M_P = 10:1, changing the R-ratio from +2.0 to –2.0 resulted in a decrease in d_γ from 15.0 nm to 11.5 nm.
  (b) using R = -2.0 and M_B/M_P = 10:1, decreasing D_B from 20 mm to 6.4 mm resulted in a decrease in d_γ from 11.5 nm to 10.1 nm.
  (c) using R = -2.0 and D_B = 20mm, increasing M_B/M_P from 5:1 to 15:1 resulted in a decrease in d_γ from 15.8 nm to 10.6 nm.

- Bulk nano-crystalline **γ**-TiAl material, in the form of a 7.6 cm x 12.7 cm x 0.53 mm thick panel, was successfully produced using a combination of ball milling, plasma spray deposition and VHP consolidation. The gamma crystallite grain size varied as follows :-
  (a) as-received powders; d_γ = 20.0 nm
  (b) ball milled powders; d_γ = 12.0 nm
  (c) plasma spray deposited; d_γ = 31.3 nm
  (d) VHP consolidated; d_γ = 90.0 nm

References

1. Y.G. Nakagawa et al., in ***Gamma Titanium Aluminides I***, TMS, Warrendale, PA, 1995, pp. 415-424.
2. P.A. Bartolotta and D.L. Krause, in ***Gamma Titanium Aluminides 1999***, TMS, Warrendale, PA, 1999, pp. 3-10.
3. C. Mercer and W.O. Soboyejo, Scripta Mater., vol.35, 1996, pp.17-22.
4. C.C. Koch and T.R. Malow, J. Metastable & Nanocrystalline Mater., vols.2-6, 1999, pp. 565-574.
5. H. Conrad and J. Narayan, Scripta Mater., vol.42, 2000, pp. 1025-1030.
6. C. Suryanarayana, Progress in Materials Science, vol.46, 2001, pp.1-184.
7. P. Bhattacharya et al., in ***Advances in Powder Metallurgy and Particulate Materials***, MPIF, Princeton, NJ, 2002, pp. 62-67.
8. O.N. Senkov et al., Scripta Mater., vol.39, 1998, pp. 691-698.
9. D.M. Dimiduk, P.L. Martin and Y.-W. Kim, J. Mater.Sci.& Engng. A, vol.A243, 1998, pp. 66-76.
10. P. LeBrun, L. Froyen and L. Delaey, J. Mater.Sci.& Engng. A, vol.A161, 1993, pp. 75-82.

Acknowledgements

Technical support for RF plasma spray deposition / VHP consolidation processing by Mr. Joel Alexa, electron micrographs by Mr. Jim Baughman and XRD measurements by Dr. Ravi Shenoy, all with Lockheed Martin Engineering and Sciences Company, Hampton, Virginia, is greatly appreciated.